TOWARDS UNSTEADY SIMULATION OF SEPARATION OF BOUNDARY LAYER

Bastien Caruelle
Service Méthodes de Calcul, AEROSPATIALE Division Airbus
316 Route de Bayonne, 31060 Toulouse, France

Frédéric Ducros
CFD-team, CERFACS
42 Avenue G. Coriolis, 31057 Toulouse Cedex, France

ABSTRACT

This paper presents unsteady simulations of an established laminar compressible boundary layer suddenly exposed to an adverse pressure gradient. The mean flow deceleration is imposed by the mean of a suction at the upper side of the computational domain. In the first part, the suction boundary condition is validated for the two dimensional laminar solution: results of Pauley et al. (1990) are recovered, and especially the threshold value of the pressure gradient for the steady separation to evolve towards an unsteady one, with periodic vortex shedding at the right frequency. In the second part, a large eddy simulation of the three dimensional case is presented and compared to the results of a quasi-equivalent direct numerical simulation performed by Spalart and Strelets (1997). Mean characteristics of the flow are recovered, and some statistics are produced. In the last part, we simulate the same case with the Spalart-Allmaras one equation turbulent model, which gives fairly good results, even though it evolves towards a steady state.

INTRODUCTION

Turbulent flow simulations involving Reynolds Averaged Navier-Stokes (RANS) are nowadays common within industrial CFD codes, and yield reasonable results when compared to experiments for a large range of steady problems. This is mainly due to the development of complex CFD tools using both efficient numerical and turbulence models (Gacherieu and Weber, 1998). However prediction of difficult phenomenon like airfoil stall or buffeting requires the development of unsteady simulations involving new tools. Recent progress in Large Eddy Simulation (LES) gives promising results (Weber et al., 1998) but clearly shows that the simulation remains too expensive for practical cases of aeronautical interests. Much effort is now devoted to achieve unsteady simulations using turbulence models derived from RANS (Spalart et al., 1997, Speziale, 1997, Ha Minh and Kourta, 1993), whereas Direct Numerical Simulation (DNS) is also used to detail turbulent separation due to adverse pressure gradient (Na and Moin, 1998).

The present paper deals with some studies carried out in that field at Aérospatiale Division Airbus. We set up an academic test case consisting of a laminar boundary layer suddenly exposed to an adverse pressure gradient (imposed by a suction at the upper boundary) leading to separation and transition to turbulence. The suction boundary condition is first validated upon the 2D laminar case treated by Pauley et al. (1990). For this flow, we propose a reference 3D LES that we compare to a quasi-equivalent DNS done by Spalart and Strelets (1997) . Results obtained in 2D with the Spalart-Allmaras model (Spalart and Allmaras, 1994) are also proposed and discussed.

CONFIGURATION - STATE OF THE ART

The sketch of the flow considered is inspired from Spalart and Strelets (1997) (see Fig. 1). It consists of a spatially developing laminar boundary layer with finite thickness at the inlet ($\delta_{1(x=0)}$) submitted to an

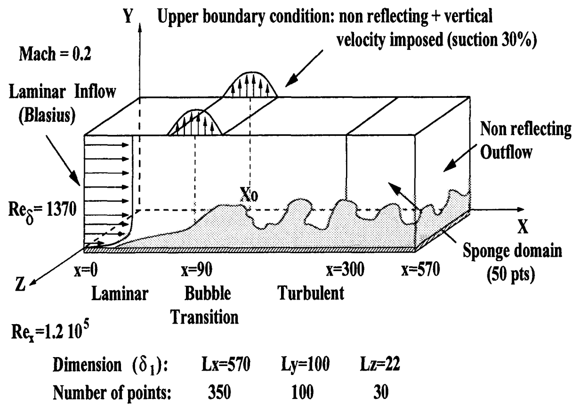

Figure 1: Test case configuration

aspiration at the upper boundary at $x = 90\delta_{1(x=0)}$, leading to an adverse pressure gradient whose strength can be measured by the factor S, defined as the fraction of the entering flow removed through the upper boundary.

Characteristics of the flow at separation are $M = 0.2$, $Re_\delta = 1730$, $Re_x = 1.2 \times 10^5$. The domain size is $L_x = 570$, $L_y = 52$, $L_z = 22$ (from here on, length are normalized with $\delta_{1(x=0)}$) with respectively $nx = 350$, $ny = 100$ and $nz = 30$ points in each direction. The resolution for the turbulent region approximatively corresponds to $\Delta_x^+ \approx 21.5$, Δ_y^+ between 1.1 and 1.5 (for the first cell), and $\Delta_z^+ \approx 16$.

Previous studies show that for the 2D laminar case the threshold value of the pressure gradient for the steady separation to evolve towards an unsteady one, with periodic vortex shedding is $S_{cr} = 12\%$. For $S > S_{cr}$, the value of Strouhal number based on the displacement thickness and local external streamwise velocity at separation is independent of the Reynolds number and equals $St_\theta = 0.00686 \pm 0.6\%$.

In the 3D incompressible case, Spalart has shown that for almost the same parameters ($Re_x = 1. \times 10^5$, L_y/L_x slightly higher), a 30% suction rate creates a separation bubble leading to transition to turbulence.

NUMERICAL TOOLS

The NSMB code

The numerical platform used for this study is a finite volume three dimensional compressible Navier-Stokes solver (NSMB, see Vos et al. (1998)), which is basically based on a second-order centered Jameson scheme. This code is currently used at AEROSPATIALE Division Airbus to get averaged Navier-Stokes solutions on full aircraft configurations using Baldwin-Lomax or SA models and the Implicit LU-SGS scheme for time marching.

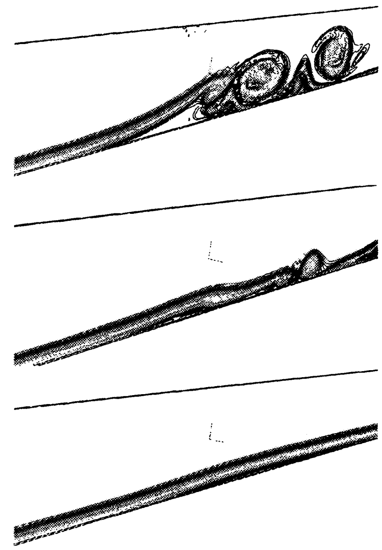

Figure 2: 2D case - vorticity magnitude for resp. S=38%, 22% and 11.5%

Turbulence treatment

The code has recently been adapted to LES, and validated for academic test cases such as freely decaying homogeneous turbulence or a temporal turbulent boundary layer (Weber et al., 1998). The sub-grid model is a wall adapted version of the filtered structure function model of Ducros et al. (1996) and proves to behave well for wall bounded turbulence and for transitional problems. The standard flux formulation is slightly modified to get better adapted spatial discretization. For the present study, an explicit fourth-order Runge-Kutta scheme with $cfl = 1$ is used.

RANS simulations are performed using the one equation Spalart-Allmaras model (we do not believe zero equation models are able to reproduce the separation). The implicit point wise treatment of source terms is removed in order to achieve the second order accuracy in time. This leads to a restriction of the time step to avoid negative values of the eddy viscosity.

Boundary Condition

The NSCBC procedure of Poinsot and Lele (1992) has been implemented in the finite volume approach. These conditions are applied at all boundaries except at the wall where no-slip condition are imposed. Periodic boundary conditions are applied in the spanwise direction. At the upper boundary, the desired suction rate ($S = 30\%$) is achieved by means of the following constraint on the characteristic variables:

$$\delta w_5 = \frac{\delta p}{\rho c} - \delta \vec{V} \cdot \vec{n} = \kappa \left(U(x, L_y, z) - V_{top}(x) \right) \quad (1)$$

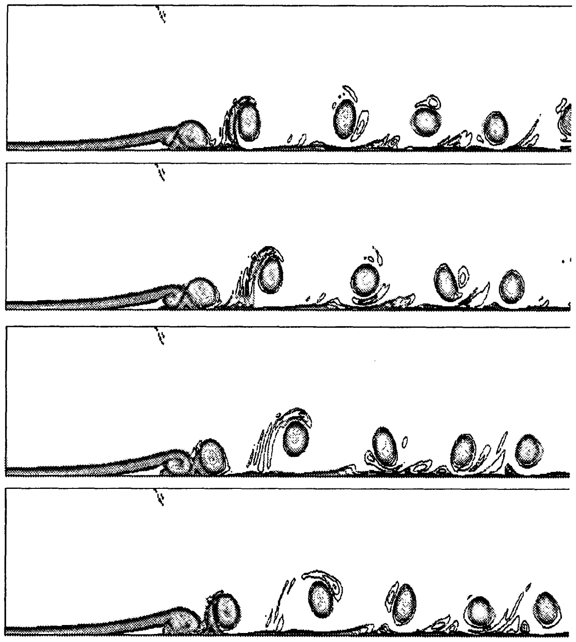

Figure 3: 2D case - Periodic vortex shedding for $S = 30\%$

where $V_{top}(x)$ is the desired vertical velocity profile:

$$V_{top}(x) = V_{blasius}(x) + \alpha e^{-\frac{1}{\beta}(x - x_{aspi})^2} \qquad (2)$$

At the outlet of the domain, non reflecting conditions are applied in combination with a sponge domain extending from $x = 300$ to the outlet at $x = 570$ containing 50 points (see Fig. 1). In this part of the domain increasing grid spacing and artificial viscosity are applied to obtain a non disturbing outlet as far as the developing adverse pressure gradient is concerned. Of course no artificial viscosity is applied in the useful region between $x = 0$ and $x = 300$

2D LAMINAR RESULTS

These simulations are done to validate the suction boundary condition. No turbulence model is used. Tests are needed to find the correct value of α (which depends on domain height) for a given S. The code is checked for adverse pressure gradients for various S. For this preliminary simulation, calculations over different grid sizes and refinements are performed (the final grid refinement in the useful region is $dx/\ \delta_1 = 1$ and $dy_{min}/\ \delta_1 = 0.008$). The results of Pauley et al. (1990), and in particular the threshold value of the suction rate between a steady separation regime and a unsteady one for higher value of S are recovered (see Fig. 2).

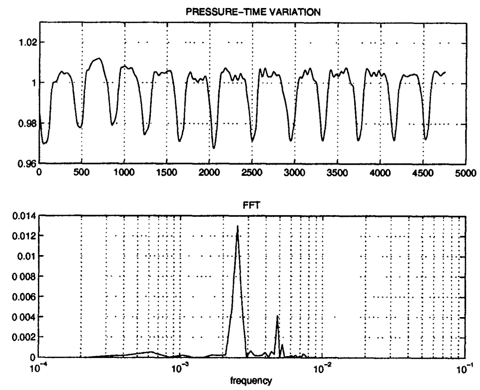

Figure 4: 2D case - frequency obtained for $S = 30\%$

Fig. 3 shows the periodic vortex shedding for $S = 30\%$ over a cycle with $dt = 80 \times \delta_1/U_{ref}$. Pressure vs time variations are recorded on a point located just after separation (Fig. 4). Periodic fluctuations are due to the vortex crossing. A Fast Fourier Transform analysis leads to a dimensionless frequency $St_\theta = f\ \theta_{sep}/Ue_{sep} = 0.0070$, which is very close to Pauley et al. (1990) results and confirms the test case set up.

3D LES RESULTS

The initial field is a converged zero pressure gradient laminar boundary layer calculation. At $t = 0$, the suction is imposed. The simulation is conducted over $t = 40000\,\delta_1/U_{ref}$, which corresponds to 21 advection times at $U_{ref} = 68ms^{-1}$.

Fig. 5 concerns a instantaneous view of the flow at $t = 35000\,\delta_1/U_{ref}$ and displays a slice of the pressure field at the upper boundary showing the suction, and two slices of vorticity, one close to the wall and the other on the rear part of the domain. Two distinct regimes appear: a steady 2D laminar region before detachment is followed by a unsteady 3D turbulent one.

Once the pressure gradient is stabilized (for $t \approx 15000\,\delta_1/U_{ref}$), we gather statistics over $t = 25000\,\delta_1/U_{ref}$. As the flow is two dimensional in the mean, all quantities are spanwise and time- averaged. A geometrical renormalization ($X = (x - x_0)\ L_y$, and $Y = y\ L_y$) is applied to have $X = 0$ at the suction location and to compare our results to the DNS.

Fig. 6 and 7 show respectively the skin friction and the pressure coefficient for DNS, LES and RANS simulations. The bubble creates a plateau of near zero values (between $X = -0.8$ and $X = 0.2$), followed by a sharp drop to negative values. The flow then reattaches ($X \approx 1$) and both coefficient increase (the adverse pressure gradient causes deceleration). When

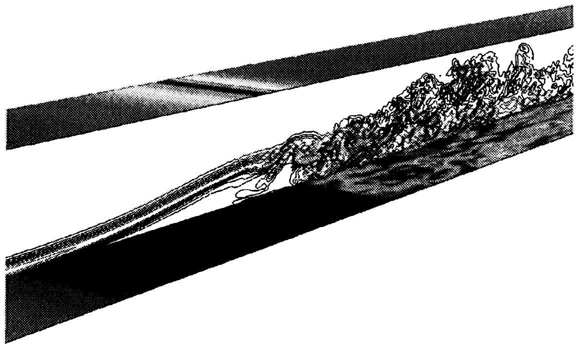

Figure 5: Instantaneous view of the flow: slices of pressure gradient (top) and vorticity (bottom and rear)

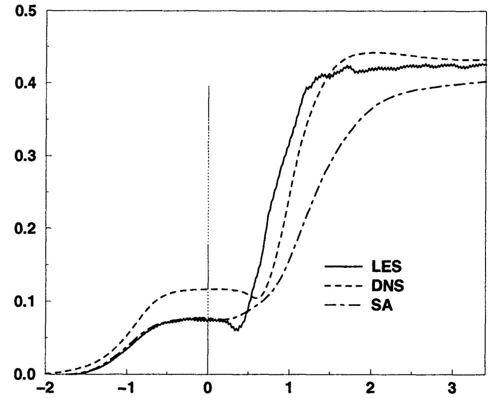

Figure 7: pressure coefficient

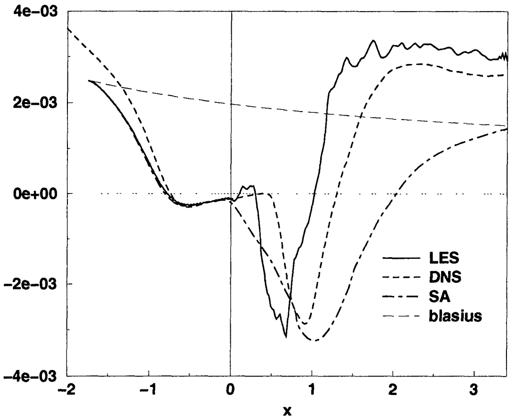

Figure 6: skin friction coefficient

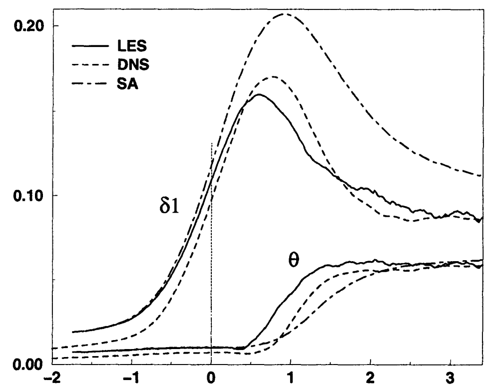

Figure 8: displacement and momentum thicknesses

compared to the DNS results, the recirculating region is a bit upstream and the Cp is underestimated for LES, but remember that simulation parameters are not exactly the same. Whereas we have the same suction rate, our taller domain height gives a larger bubble.

Fig. 8 show momentum and displacement thicknesses. When the flow undergoes separation, a rapid rise is observed, followed by a plateau at a lower value in the turbulent reattached region. The shape factor H (Fig. 14) is falling from 2.61 at the inlet to 1.49 after reattachment. In the laminar region, δ_1 and θ are not equivalent upstream of separation for LES and DNS, due to a larger Re_x in our case.

Examination of mean velocity profiles (Fig. 9) exhibits a modified log law (U^+ at $y^+ = 100$ lower than 15) compatible with formerly obtained results for a turbulent boundary layer under adverse pressure gradient (Alams and Sandham, 1998). After transition within the bubble, the flow is slowly relaxing towards equilibrium (reached for $x = 436$).

Fig. 10 shows mean velocity and u_{rms} profiles before and within the bubble for $x = 196, 216, 241, 286$, each normalized by its local maximum. Rms fluctuations are confined in the boundary layer. In the laminar region, maximum u_{rms} values are above 0.1% and rise up to 22% at $x = 241$. w_{rms} grows by a factor of 20 up to 17% indicating the three-dimensionality of the flow.

Eddy-viscosity profiles are presented Fig. 11. The sub-grid stress model is more active just after separation than in the developed turbulent boundary layer. Instantaneous maximum values are about twenty times the flow viscosity, whereas mean value are between one and three times this value. A similar ratio was found by Weber et al. (1998) for the LES around the Aérospatiale A-Profile.

We believe we have obtained a good quality LES simulation of this flow, which can now be used as a reference to test unsteady RANS models.

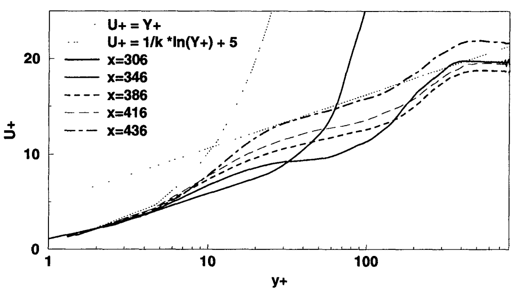

Figure 9: Mean streamwise velocity profiles in wall unit (LES)

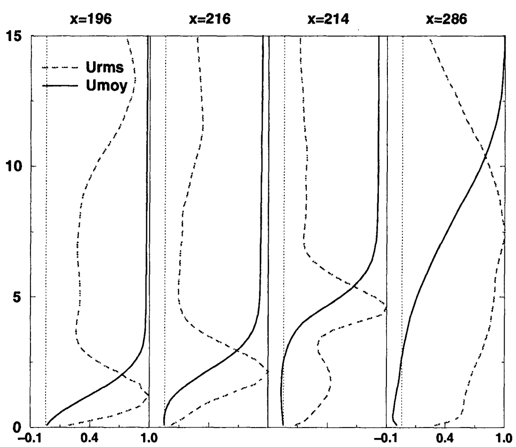

Figure 10: Mean velocity and u_{rms} profiles (LES)

RANS RESULTS

RANS simulation is performed over the same grid using the Spalart-Allmaras model. Steady and unsteady simulations (with resp. implicit or explicit time-stepping) give almost the same solution: a steady separated region is found, with no unsteady features. Transition is not specified: zero values of ν_t are prescribed at inlet and at the wall. The flow remains laminar before separation since $\nu_t = 0$ is a stable solution of the turbulent transport equation.

The LES results are now taken as reference. Boundary layer parameters are presented Fig. 6, 7 and 8. The model behaves well until $X = 0$. The skin friction coefficient starts falling too early, and the size of the separated region is overestimated: The C_F recovers positive value for $X = 2$ ($C_F > 0$ for $X \doteq 1$ in the LES). The pressure coefficient is underestimated within the separated region. The displacement thickness is too high, and the momentum thickness grows too slowly.

Eddy-viscosity profiles (Fig. 11) show that the SA simulation is much more dissipative than the LES, since large eddies are directly resolved in this latter

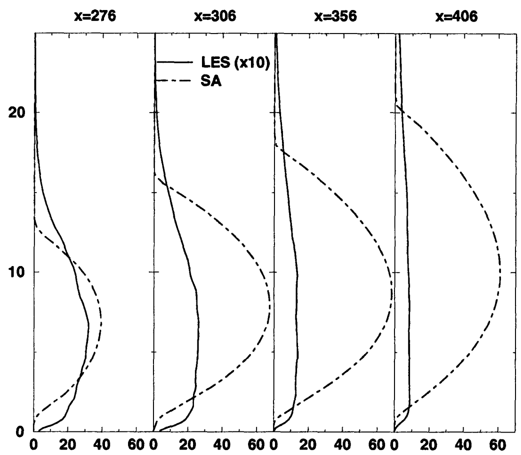

Figure 11: Mean eddy-viscosity profiles normalized by fluid viscosity (LES and SA)

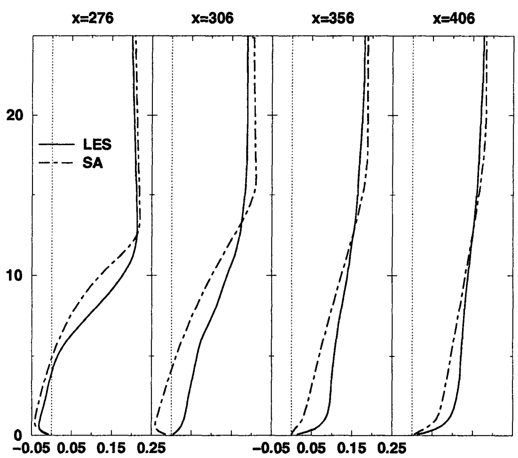

Figure 12: Mean velocity profiles (LES et SA)

case, whereas they are taken into account in the eddy-viscosity for the RANS. This may explain why unsteady RANS simulation remains steady.

Mean velocity profiles are proposed Fig. 12. We see that the flow is still detached for $x = 306$, whereas it is already re-attached in LES. Fig. 13 shows the mean velocity magnitude field for LES (top) and SA (bottom). The RANS boundary layer is too thick downstream of the separated region. Even if RANS eddy-viscosity is sixty times the LES one, the boundary layer is not fully developed: the shape factor is still too high ($H = 1.85$) at the end of the useful domain and still decreases (Fig. 14). For LES and DNS, it is already stabilized around 1.45 at $X = 2.35$.

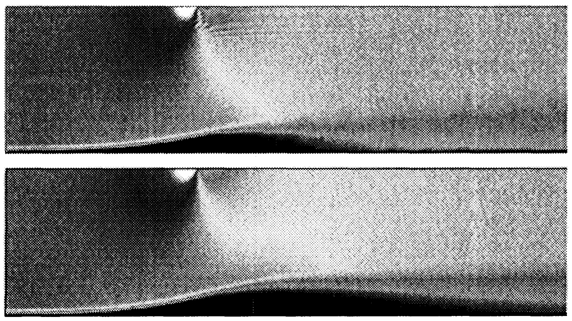

Figure 13: View of the mean velocity magnitude for resp. LES and SA

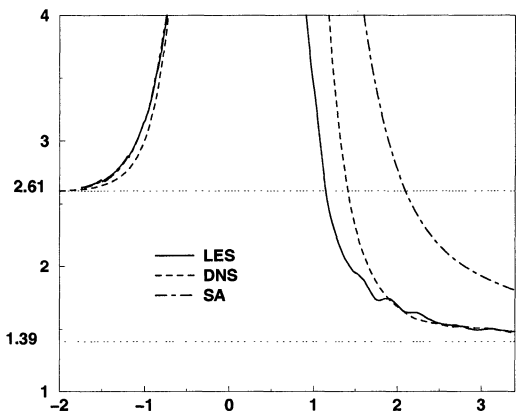

Figure 14: Shape factor (LES, DNS and SA)

CONCLUSION

We have set up a reference test case for unsteady RANS simulation. The suction boundary condition has been successfully validated in the two-dimensional laminar case. The three-dimensional Large Eddy Simulation results are globally satisfying: main features of the flow (separation, transition and relaxation towards an equilibrium turbulent boundary layer) are faithfully recovered.

SA results are not far from LES, but can clearly be ameliorated. In a future work, we intend to test this model upon less stretched grids. Other turbulent model will be investigated on the same case, such as the $k-\epsilon$ family, together with the concept of "Detached Eddy Simulation " of Spalart et al. (1997). The best model will be retained to simulate more complex three-dimensional geometries.

Acknowledgments: The LES has been done on the Fujitsu VPP-700 of Météo-France. We also acknowledge P. Spalart for making available his DNS results.

REFERENCES

Alam, M. and Sandham, N.D., 1998 "Numerical Study of Separation Bubbles with Turbulent Reattachment followed by a Boundary Layer Relaxation", in *Parallel Computational Fluid Dynamics*, pp. 571-578.

Ducros F., Comte P., and Lesieur M., 1996, "Large-eddy simulation of transition to turbulence in a weakly-compressible boundary layer over a flat plate", *Journal of Fluid Mechanics*, Vol. 326, pp. 1-36.

Gacherieu, C., and Weber, C., 1998, "Assessment of Algebraic and one-equation turbulence models for the transonic turbulent flow around a full aircraft configuration", in *29th AIAA Fluid Dynamics Conference*, June 18, Albuquerque, AIAA 98-2737.

Ha Minh, H., and Kourta, A., 1993, "Semi-deterministic turbulence modeling for flows dominated by strong organized structures", in *9th Symposium on Turbulent Shear Flows*, Kyoto, No. 10-5.

Na, Y., and Moin, P., 1998, "Direct numerical simulation of separated turbulent boundary layer", *Journal of Fluid Mechanics*, Vol. 374, pp. 379-405.

Pauley, L.L., Moin , P., and Reynolds, W.C., 1990 "The Structure of Two-dimensionnal Separation", *Journal of Fluid Mechanics*, Vol. 220. pp. 397-411.

Poinsot, T., and Lele, S. K., 1992, "Boundary Conditions for Direct Simulations of Compressible Viscous Flows", *Journal of Computational Physics*, Vol. 101. pp. 104-128.

Speziale, G., 1997, "Turbulence modeling for time-dependant RANS and VLES: a review", *AIAA paper*, No. AIAA-97-2051.

Spalart, P.R., Jou, W-H, Strelets, M., and Allmaras, S. R., 1997, "Comments on the feasibility of LES for wings, and on a hybrid RANS/LES approach", in *1st AFOSR Int. Conf. on DNS/LES*, Ruston (LA), Greyden Press.

Spalart, P. R., and Strelets, M. K., 1997, "Direct and Reynolds-averaged numerical simulations of a transitional separation bubble", in *11th Symposium on Turbulent Shear Flow*, Grenoble, 8-10 Sept. 97.

Spalart, P. R. and Allmaras, S. R., 1994, "A one-equation turbulence model for aerodynamic flows", *La recherche Aérospatiale*, No.1 , pp. 5-21.

Vos, J. B., Rizzi, A. W., Corjon, A., Chaput, E., and Soinne, E., 1998, "Recent advances in aerodynamics inside the NSMB (Navier Stokes multi block) consortium", in *36th Aerospace Sciences Meeting and Exhibit*, Jan. 12-15, No. AIAA 98-0225.

Weber, C., Ducros, F., and Corjon, A., 1998, "Large eddy simulation of complex turbulent flow", in *29th AIAA Fluid Dynamics Conference*, June 18, Albuquerque, AIAA 98-2651.